



# Sustained delivery of rhMG53 promotes diabetic wound healing and hair follicle development

Hong Niu<sup>a,b,1</sup>, Haichang Li<sup>c,1</sup>, Ya Guan<sup>a,b,1</sup>, Xin Zhou<sup>c,d</sup>, Zhongguang Li<sup>c</sup>, Serana Li Zhao<sup>c</sup>, Peng Chen<sup>c</sup>, Tao Tan<sup>c</sup>, Hua Zhu<sup>c</sup>, Valerie Bergdall<sup>e</sup>, Xuehong Xu<sup>d</sup>, Jianjie Ma<sup>c,\*\*</sup>, Jianjun Guan<sup>a,b,\*</sup>

<sup>a</sup> Department of Mechanical Engineering and Materials Science, Washington University in St. Louis, St. Louis, MO, 63130, USA

<sup>b</sup> Institute of Materials Science and Engineering, Washington University in St. Louis, St. Louis, MO, 63130, USA

<sup>c</sup> Department of Surgery, Davis Heart and Lung Research Institute, The Ohio State University, Columbus, OH, 43210, USA

<sup>d</sup> Laboratory of Cell Genetics and Developmental Biology, Shaanxi Normal University College of Life Sciences, Xi'an, 710062, China

<sup>e</sup> Department of Veterinary Preventive Medicine, University Laboratory Animals Resources, The Ohio State University, Columbus, OH, 43210, USA

## ARTICLE INFO

### Keywords:

Diabetic wound healing  
hair follicle stem cell  
MG53  
ROS-Scavenging hydrogel  
Controlled drug delivery

## ABSTRACT

MG53 is an essential component of the cell membrane repair machinery, participating in the healing of dermal wounds. Here we develop a novel delivery system using recombinant human MG53 (rhMG53) protein and a reactive oxygen species (ROS)-scavenging gel to treat diabetic wounds. Mice with ablation of MG53 display defective hair follicle structure, and topical application of rhMG53 can promote hair growth in the *mg53*<sup>-/-</sup> mice. Cell lineage tracing studies reveal a physiological function of MG53 in modulating the proliferation of hair follicle stem cells (HFSCs). We find that rhMG53 protects HFSCs from oxidative stress-induced apoptosis and stimulates differentiation of HFSCs into keratinocytes. The cytoprotective function of MG53 is mediated by STATs and MAPK signaling in HFSCs. The thermosensitive ROS-scavenging gel encapsulated with rhMG53 allows for sustained release of rhMG53 and promotes healing of chronic cutaneous wounds and hair follicle development in the *db/db* mice. These findings support the potential therapeutic value of using rhMG53 in combination with ROS-scavenging gel to treat diabetic wounds.

## 1. Introduction

Chronic wounds are a major challenge to public health. An aging population combined with an increase in cardiovascular and metabolic diseases contribute to a growing burden of chronic wound management [1–3]. Chronic wounds impair skin and tissue homeostasis. The healing is a complex process consisting of four stages, including blood clotting (hemostasis), inflammation, tissue growth (proliferation), and tissue remodeling (maturation). Various types of skin cells, multiple growth factors, cytokines, and oxidative stress are involved in this process [4–10].

A major cause of non-healing chronic wounds is the inability of skin stem cells to effectively activate or differentiate [11]. To revert the situation, many therapies have targeted epidermal stem cells (ESCs), a

crucial cell type for skin regeneration [12–14]. ESCs have the ability to regenerate epidermis, and if activated adequately, develop into different skin cell types. Hair follicle stem cells (HFSCs), which are multipotent stem cells of the epidermis, contribute to the formation and differentiation of the functional epidermis during normal development and wound healing [15–17]. Studies from animals and humans have revealed that HFSCs are the major reservoir of adult stem cells [18,19]. It has been shown that transplantation of human hair follicle grafting into the wound beds enhanced epithelialization and dermal reorganization, thus promoting healing of chronic ulcers [20]. Using a genetically engineered mouse model, Ito et al. demonstrate that HFSCs can migrate to the epidermal defect and stimulate re-epithelialization, angiogenesis, and dermal regeneration [21]. However, the functions of HFSCs are largely compromised due to an increase of reactive oxygen species (ROS) associated with impaired chronic wounds. Many studies

Peer review under responsibility of KeAi Communications Co., Ltd.

\* Corresponding author. Department of Mechanical Engineering and Materials Science, Washington University in St. Louis, St. Louis, MO, 63130, USA.

\*\* Corresponding author.

E-mail addresses: [Jianjie.Ma@osumc.edu](mailto:Jianjie.Ma@osumc.edu) (J. Ma), [jguan22@wustl.edu](mailto:jguan22@wustl.edu) (J. Guan).

<sup>1</sup> These authors contributed equally to this work.

<https://doi.org/10.1016/j.bioactmat.2022.03.017>

Received 24 January 2022; Received in revised form 7 March 2022; Accepted 11 March 2022

Available online 16 March 2022

2452-199X/© 2022 The Authors. Publishing services by Elsevier B.V. on behalf of KeAi Communications Co. Ltd. This is an open access article under the CC BY-NC-ND license (<http://creativecommons.org/licenses/by-nc-nd/4.0/>).

### Abbreviations

HFSCs	Human hair follicle stem cells
rhMG53	Recombinant human MG53 protein
HPPE	4-(Hydroxymethyl)-phenylboronic acid pinacol ester
TEA	Triethylamine
BPO	Benzoyl peroxide
AHPPE	Acrylation of HPPE
HEMA	2-Hydroxyethyl methacrylate
DPBS	Dulbecco's phosphate-buffered saline
DI	Deionized water
MTT	3-(4,5-Dimethylthiazol-2-yl)-2,5-diphenyltetrazolium bromide
STAT3	Signal transducer and activator of transcription 3
MAPK	Mitogen-activated protein kinase
ROS	Reactive oxygen species
TRIM	Tripartite motif

showed that proper control of ROS is required for defending pathogens and mediating cellular signaling pathways [22]. However, elevated and sustained ROS leads to lipid peroxidation that further damages cell membrane [23], which has been implicated in dysfunction of HFSCs associated with chronic wounds [24].

MG53, a tripartite motif (TRIM) family protein, has been identified as an essential component of the cell membrane repair machinery, and genetic ablation of MG53 results in defective membrane repair and tissue regenerative capacity [25]. We have shown that the recombinant human MG53 (rhMG53) protein can promote wound healing when tested on non-diabetic conditions [26–32]. However, it remains unclear how MG53 affects the healing of diabetic wounds with upregulated ROS content, as well as its role in regulating HFSC survival and differentiation under such oxidative stress conditions. In addition, rhMG53 has a short half-life, and direct administration of MG53 to the wound site or intravascular injection may have low efficacy [33,34].

To increase therapeutic efficacy of proteins in wound healing, hydrogels have been used as delivery vehicles as they allow the proteins to gradually release out. In addition, hydrogels have tissue-like mechanical properties, and can provide a moist environment to the wounds [35,36]. Among different hydrogels, multifunctional hydrogels with anti-inflammation and antioxidant properties are attractive for healing diabetic wounds that are featured by prolonged inflammation and excessive ROS content [35,36].

In this work, we investigated the effect of MG53 on HFSC survival and differentiation under ROS condition, and the role of MG53 in hair follicle development. We also developed an injectable, thermosensitive, and ROS-scavenging hydrogel for controlled release of rhMG53 in diabetic wounds. We tested the effect of the rhMG53 delivery system on diabetic wound closure and hair follicle development.

## 2. Materials and methods

### 2.1. Chemicals

All chemicals were obtained from Sigma-Aldrich unless otherwise described. N-Isopropylacrylamide (NIPAAm, TCI) was recrystallized in hexane 3 times before use. 2-Hydroxyethyl methacrylate (HEMA, Alfa Aesar) was used after passing through a column filled with inhibitor removers. Benzoyl peroxide (BPO, Fisher Scientific) was freeze-dried before polymerization. Acryloyl chloride (Sigma), 4-(hydroxymethyl)-phenylboronic acid pinacol ester (Sigma-Aldrich, HPPE), triethylamine (TEA, VWR), and hydrogen peroxide (H<sub>2</sub>O<sub>2</sub>) (30%, Sigma-Aldrich) were used as received. rhMG53 protein was purified from *E. coli* fermentation as described previously [33].

### 2.2. Animal care and wound healing models

All animal care and usage followed NIH guidelines and were approved by IACUC of The Ohio State University. *mg53*<sup>-/-</sup> mice and wild-type littermates were bred and generated as previously described [28]. C57BL/6 mice, *db/db* (B6.BKS(D)-*Lep<sup>db</sup>/J*, mouse strain: 000697), and *db/+* littermate were purchased from the Jackson laboratory.

**Hair growth study:** Hair growth assay was performed for both unwounded and wounded mice. For unwounded mice, dorsal hair was shaved using electric clippers, and cleaned by hair remover lotion Nair™ (Church and Dwight Co., Inc, NJ). For wounded mice, the wounds were created as previously described [37]. Briefly, following shaving and cleaning dorsal hair, the exposed skin was disinfected by the application of betadine solution. Full thickness dermal wounds were created using 5 mm biopsy punches (Integra™ Miltex®). The mice then received a subcutaneous injection of either 200 μL saline (as control) or rhMG53 (2 mg/kg). The treatments were performed daily for 7 successive days. Hair growth was monitored, and images were taken at pre-determined time points.

**Chronic wound study:** 10-week-old female BKS *db/db* mice were anesthetized using isoflurane, followed by dorsal hair removal and disinfection. Two full-thickness wounds were created using a 5 mm biopsy punch (Integra™ Miltex®) on each mouse. Wounds were left open, and then received 200 μL hydrogel solution, or 200 μL rhMG53/hydrogel solution via topical application. *db/db* mice injected with saline each day, *db/db* mice without treatment, and *db/+* mice without treatment were used as control groups. The wound images were taken at each time point. The wound size was calculated using ImageJ [38], and normalized to that on day 0.

### 2.3. HFSCs cell culture and rhMG53 uptake

Human hair follicle stem cells (HFSCs) were obtained from Celprogen. The cells were positive to markers such as Keratin 15, Keratin 19, CD34, and CD133. The cells were cultured on an expansion extracellular matrix using complete media (Celprogen) supplemented with 1% penicillin/streptomycin at 37 °C in a humidified atmosphere of 5% CO<sub>2</sub>. The cells at passages 3–8 were used for the studies.

rhMG53 protein and bovine serum albumin (BSA) were labeled with Alexa Fluor™ 647 protein labeling kit (Invitrogen™, A20173) according to the manufacturer's instructions. HFSCs were then cultured on glass-bottom dishes (MatTek Inc.) followed by adding Alex647-rhMG53. Live cell images were taken by Nikon A1R confocal microscope and analyzed using ImageJ software. Alex647 labeled BSA was used as control.

### 2.4. Lineage tracing assay for epithelial stem cells

R26R-Confetti transgenic mice (Strain #013731, Jackson laboratory) were crossed with K14Cre<sup>ERT2</sup> mice (strain #005107, Jackson laboratory) to obtain R26R-Confetti/K14Cre<sup>ERT2</sup> mice, which were used in this study for lineage tracing of skin epithelial stem cells [39,40]. The Brainbow2.1 cassette included a head-to-tail LoxP-flanked dimer of nuclear-localized green fluorescent protein (GFP) with a reverse-oriented cytoplasmic yellow fluorescent protein (YFP), and a dimer of cytoplasmic red fluorescent protein (RFP) with a reverse-oriented membrane-tethered cyan fluorescent protein (CFP). The mice were then crossed with *mg53*<sup>-/-</sup> mice. Cre activity was induced by tamoxifen (dissociated in corn oil, 1 mg/day) for 5 consecutive days. A 1-mm ear hole was made in the center of the ear of mice using a metal ear puncher (Fisher Scientific, Cat. No 50822358) as described previously [41]. The wounds were monitored daily. The multi-channel images were acquired using a Nikon Eclipse Ti2 microscope with 10 × 0.45 objective. The ImageJ software was used for image analysis.

## 2.5. Effect of rhMG53 on HFSC apoptosis under oxidative stress

TUNEL assay was performed to determine the effect of rhMG53 on reducing cell apoptosis. HFSCs were seeded on glass slides inserted in a 6-well plate at a density of  $1 \times 10^5$  cells/mL. After 12 h, 800  $\mu$ L of serum-free basal medium alone (control), rhMG53 solution (10  $\mu$ g/mL), H<sub>2</sub>O<sub>2</sub> (500  $\mu$ M), and rhMG53/H<sub>2</sub>O<sub>2</sub> was added, respectively. Following 24 h of culture, TUNEL assay (Abcam) was performed, and images were taken using an optical microscope.

## 2.6. Effect of rhMG53 on HFSC differentiation under oxidative stress

For the HFSCs differentiation study, the cells were seeded in a 24-well plate to reach a confluency of 30–40%. The HFSCs were then treated with 500  $\mu$ L of serum-free basal medium (control), rhMG53 solution (10  $\mu$ g/mL), H<sub>2</sub>O<sub>2</sub> (500  $\mu$ M), and rhMG53/H<sub>2</sub>O<sub>2</sub> respectively for 48 h ( $n = 5$ ). After fixation with 4% paraformaldehyde, the cells were incubated with rabbit monoclonal anti-cytokeratin 10 (K10, Abcam) overnight at 4 °C, followed by corresponding secondary antibody. DAPI was used to stain the nuclei. The cells were imaged by an Olympus confocal microscope. At least 8 images were taken for each well.

## 2.7. Western blotting analysis

Primary antibodies used in this study are as follows: anti-GAPDH (Abcam), phosphor-anti-STAT3 (p-STAT3, Abcam), STAT3 antibody (R&D systems), phospho-MAPK<sub>p42/44</sub> (p-Erk1/2, Cell signaling) and MAPK<sub>p42/44</sub> (Erk1/2, Cell signaling). Protein lysates were collected from HFSCs treated with indicated groups and separated by sodium dodecyl-sulfate polyacrylamide gel electrophoresis (SDS-PAGE). Low fluorescence polyvinylidene difluoride (LF-PVDF) membranes (Bio-rad) were used to transfer the proteins at 4 °C overnight, followed by 20-min blocking, and incubation with primary antibodies overnight with continuous shaking at 4 °C. The blots were washed with PBST (DPBS+0.1% Tween 20) 3 times and incubated with appropriate horseradish peroxidase (HRP)-conjugated secondary antibodies. Immunoblots were detected by a detection kit from Advansta and imaged using ChemiDoc XRS + System (Bio-rad).

## 2.8. Hydrogel preparation

ROS-sensitive hydrogel was synthesized by free radical polymerization of NIPAAm, HEMA and acrylated HPPE (AHPPE) using BPO as an initiator [38,42,43]. The molar feed ratio was 79/15/6 (abbreviated as ROSS-A6). The control ROS-insensitive hydrogel was synthesized by polymerization of NIPAAm, HEMA and acrylate-poly lactide with molar feed ratio of 86/10/4 using the same approach. The hydrogel was abbreviated as ROSIS. Chemical structures of the synthesized hydrogels were confirmed by <sup>1</sup>H NMR spectra.

## 2.9. Hydrogel characterization and rhMG53 encapsulation

Hydrogel solution (6 wt%) was prepared by dissolving the dry polymer in DPBS at 4 °C. Rheological properties of the solution was tested in a HR-20 rheometer equipped with a temperature controllable Peltier plate. A 20-mm smooth cone geometry was used during the test. The temperature was swept from 4 °C to 40 °C at a rate of 1 °C/min. The fixed strain and frequency were 2%, and 1 Hz, respectively. The storage modulus  $G'$  and loss modulus  $G''$  and  $\tan \delta$  were collected and analyzed by TA Rheology Advantage™ software. The viscosity was measured at 4 °C with a continuous ramp of shear rates from 1 to 50  $s^{-1}$ .

To encapsulate rhMG53, stock solution of the protein (10 mg/mL) was mixed with the hydrogel solution, and stirred for 6 h. The final rhMG53 concentration was 2 mg/mL. Gelation time of the mixture was tested at 37 °C using a microscope equipped with a temperature controllable system (Olympus, IX71 with Weather Station). The gelation

time was defined as the time allowing for the 4 °C mixture to become completely opaque at 37 °C [43,44]. Injectability of the mixture was tested by injecting the 4 °C mixture through a 27G needle, which is typically used for tissue injection.

## 2.10. Release kinetics of rhMG53

For release kinetics study, 200  $\mu$ L of the above rhMG53 and hydrogel mixture was transferred into a 1.5 mL centrifuge tube. The mixture was incubated at 37 °C for 4 h to reach water equilibrium. The supernatant was then removed and replaced by 200  $\mu$ L release medium (DPBS with 1% penicillin/streptomycin). At days 1, 3, 7, 14, and 21, the release medium was collected, and the fresh release medium was added. The concentration of released rhMG53 was determined by Bradford protein assay.

## 2.11. HFSC survival on the ROS-sensitive hydrogel under oxidative stress

ROSS-A6 gel and ROSIS gel were cast at the bottom of wells in a 96-well plate, respectively. HFSCs were seeded on the hydrogels at a density of 5000 cells/well. After 1 day of culture, 200  $\mu$ L medium with or without H<sub>2</sub>O<sub>2</sub> (500  $\mu$ M) were added into each well. The cells were cultured for 5 days. MTT assay was then performed to assess the cell viability [45]. To visualize HFSCs, the cells were pre-labeled with live cell tracker CM-Dil (Invitrogen) prior to seeding. The cells were imaged using Olympus confocal microscopy.

## 2.12. Histology and immunofluorescence analysis

Histology and immunofluorescence analysis were performed as previously described [37]. Briefly, the skin samples were dissected from the animals at the indicated time points and fixed in 4% paraformaldehyde overnight. The samples were embedded in paraffin and cut into 5- $\mu$ m thick sections. For histological analysis, Masson's trichrome staining was performed on the sections. For immunohistochemical staining, the tissue sections were stained with mouse monoclonal anti-cytokeratin 14 (Abcam). Cell nuclei were stained with DAPI (Sigma).

## 2.13. Statistical analysis

All data are expressed as means  $\pm$  standard deviation unless otherwise specified. Statistical evaluation was conducted using the Student's t-tests for comparisons between two groups and by ANOVA for comparisons among more than two groups. A value of  $p < 0.05$  was considered statistically significant.

## 3. Results and discussion

### 3.1. MG53 deficiency causes defective hair follicle structure and hair growth

Previously, we have shown that *mg53*<sup>-/-</sup> mice display delayed healing and abnormal scarring following cutaneous injuries [37]. Interestingly, histological analysis revealed defective hair follicle structure in skin derived from *mg53*<sup>-/-</sup> mice when compared with the wild type (WT) mice (Fig. 1a and b). To further test whether MG53 is involved in hair follicle development, hair was shaved in the back region of *mg53*<sup>-/-</sup> and WT mice using electric clippers and cleared by Nair™ (hair remover lotion) (Fig. 1c). The hair growth was monitored, and images were taken at indicated time points. We found the hair growth is slower in *mg53*<sup>-/-</sup> mice compared with WT at 12-day post hair removal (Fig. 1c). Further, we tested the effect of rhMG53 in hair growth using *mg53*<sup>-/-</sup> mice. After hair removal, the mice were treated with a subcutaneous injection of either 200  $\mu$ L saline (as control) or rhMG53 (2 mg/kg) daily for 7 successive days. Improved hair growth was clearly



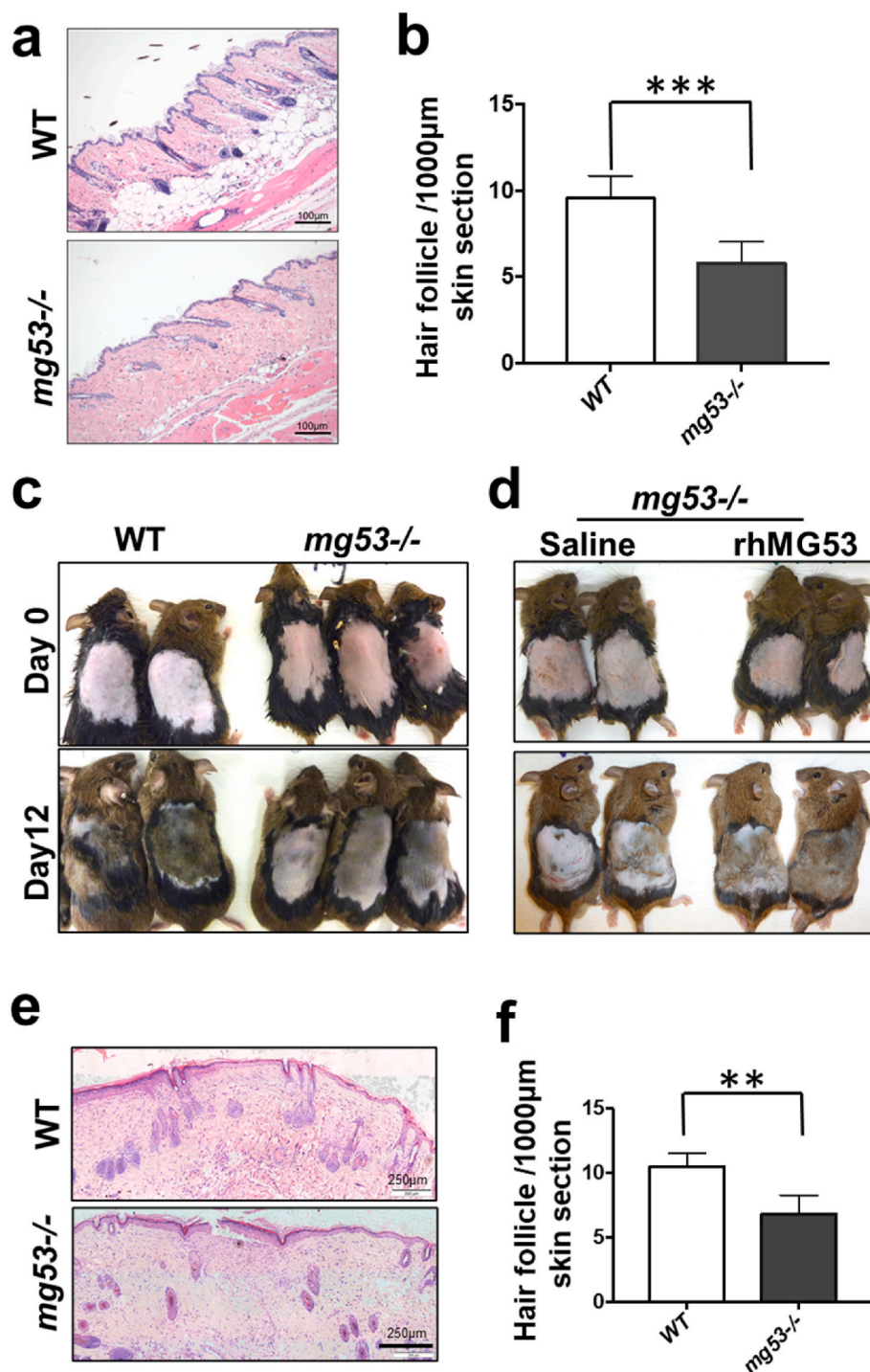


**Fig. 1.** Knockout of MG53 causes defects in hair follicle development. **a.** H&E staining showed defective hair follicle development in  $mg53^{-/-}$  mice on back skin compared with WT. **b.** Reduced hair follicles in  $mg53^{-/-}$  skin compared to WT skin. \*\*\* $p < 0.001$  ( $n = 12$ ). Representative images of hair growth in  $mg53^{-/-}$  mice compared with WT control (c), and the hair growth compared with the rhMG53 treatment (d). **e.** Two full thickness dermal wounds were created using sterile  $\phi$  4 mm biopsy punches (Integra™ Miltex®). Skin samples were harvested and stained with Hematoxylin-Eosin (H&E) at different time points. **f.** Quantification shows reduced hair follicles in  $mg53^{-/-}$  skin compared with WT skin at day 7 after wound. \*\* $p < 0.01$  ( $n = 10$ ).

observed in rhMG53-treated mice compared to saline-treated mice at day 12 (Fig. 1d). These data suggest that genetic ablation of MG53 leads to abnormal hair follicle development, and the administration of rhMG53 provides beneficial effects on hair growth.

The wound healing process involves migration of fibroblasts to wound sites and differentiation of fibroblasts into myofibroblasts [4–8]. Hair follicle stem cells (HFSCs) have been shown to play important roles in the healing process. We next evaluated the role of MG53 in hair follicle development following wounds using an established excisional cutaneous wounding model as described in our previous studies [37,46]. H&E staining confirmed that a significantly reduced hair follicle number in the  $mg53^{-/-}$  mice compared to the WT mice at day 7 post wounds

(Fig. 1e and f). These data reveal a role for MG53 in hair follicle development, which may contribute to wound healing.

### 3.2. Loss-of-function of MG53 impairs skin epithelial stem cell migration and differentiation during wound healing

Emerging evidence has demonstrated that therapy targeting stem cells represents one promising direction in the treatment of chronic wounds [47]. We have recently shown that mice with sustained elevation of MG53 in the bloodstream display enhanced tissue regenerative capacity following wound or injury, which was associated with increased proliferation of stem cells [41,48]. To evaluate whether MG53



modulates the *in vivo* function of epithelial stem cells associated with dermal injury, we performed a lineage tracing study using an inducible Cre line that targets epidermal stem cells (K14 driven) in combination with the Rainbow reporter (R26R-Confetti/K14Cre<sup>ERT</sup> Brainbow multi-color transgenic mice). The lineage tracing model allows the tracking of the progeny of K14 positive cells [49,50]. The Brainbow mice were further crossed with the *mg53*<sup>-/-</sup> mice to generate the Brainbow *mg53*<sup>-/-</sup> mice. After tamoxifen-induced Cre recombinase activity, a 1-mm full-thickness wound was made in the center of the ear as described previously [41]. The multi-color fluorescent images were

taken at different days post ear-punch injury (Fig. 2a). The colonies of epidermal stem cells were analyzed at indicated time points (Fig. 2b and c). As expected, the colon number of epithelial stem cells increased over time following wound healing. However, the *mg53*<sup>-/-</sup> mice displayed delayed wound healing and significantly reduced stem cell clones compared to WT littermates at the same time point (Fig. 2c). These observations provide strong support for MG53’s role in modulating the *in vivo* function of epithelial stem cells following dermal wounds.

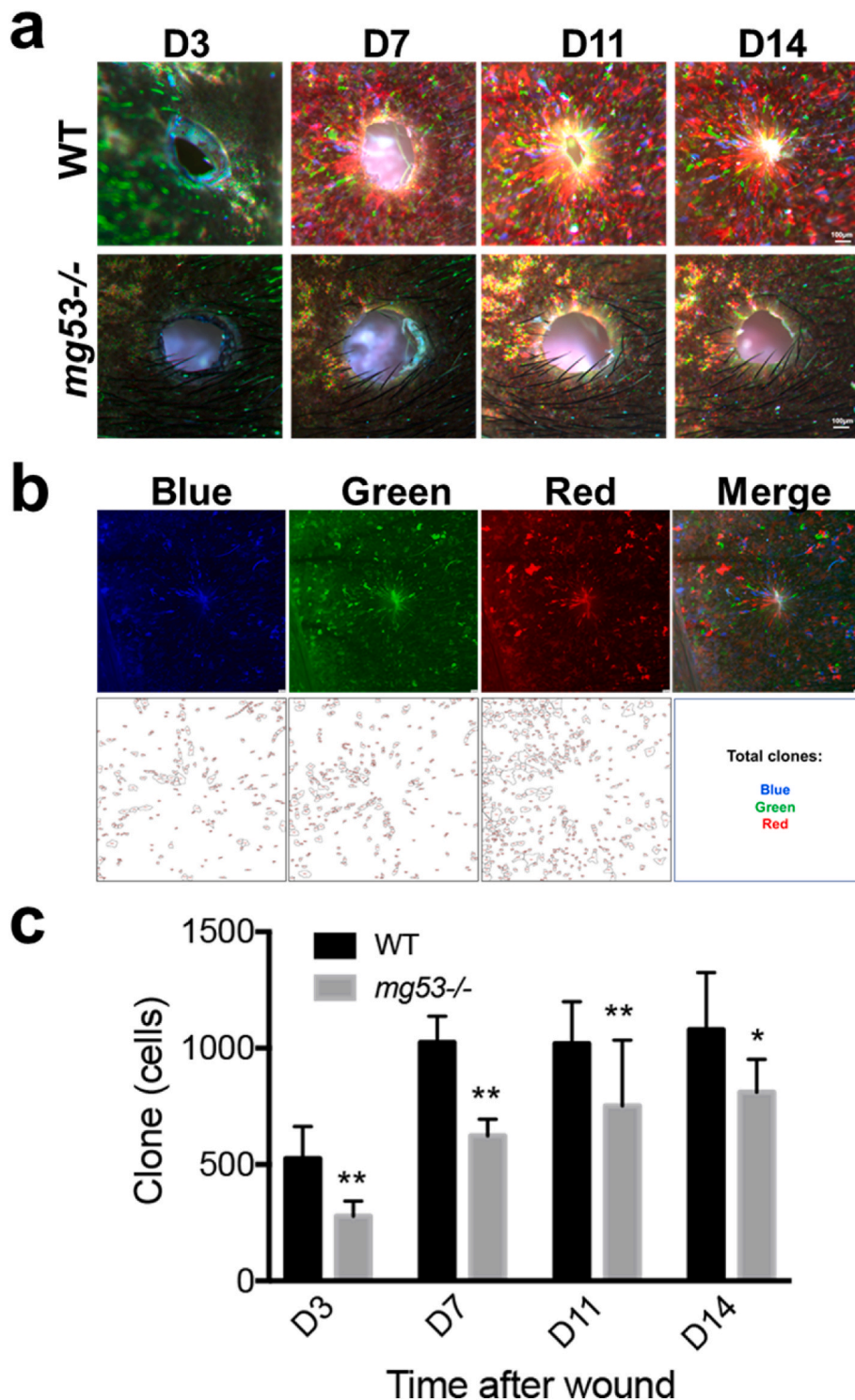


**Fig. 2. MG53 enhances epithelial stem cell migration and differentiation during wound healing.** a. Representative images of ear wound from Brainbow *mg53*<sup>-/-</sup> and Brainbow WT mice at different time points. b. Illustration of the multi-color and analysis of induced epidermal clones with Brainbow transgenic mice. c. Statistical analyses revealed that *mg53*<sup>-/-</sup> mice displayed comprised wound healing and reduced epithelial stem cell clones compared with WT mice at the indicated time points. \*\*p < 0.01; \*p < 0.05 (n = 3/group).

3.3. rhMG53 promotes HFSCs survival and differentiation under oxidative stress

In wound healing, ROS acts as a critical regulator at a low concentration (100–250  $\mu\text{M}$ ) [51,52]. Yet the upregulated ROS in chronic diabetic wounds results in skin cell death [53], and malfunction of stem

cells [54], thus prolonging the pro-inflammatory response and delaying the healing process. Previous studies have shown that rhMG53 protects various types of cells from membrane disruption, and can enhance cell survival [48]. We tested the potential protective effect of rhMG53 on HFSCs, a key type of skin epithelial stem cells for hair follicle development and wound closure. First, we determined whether rhMG53 can

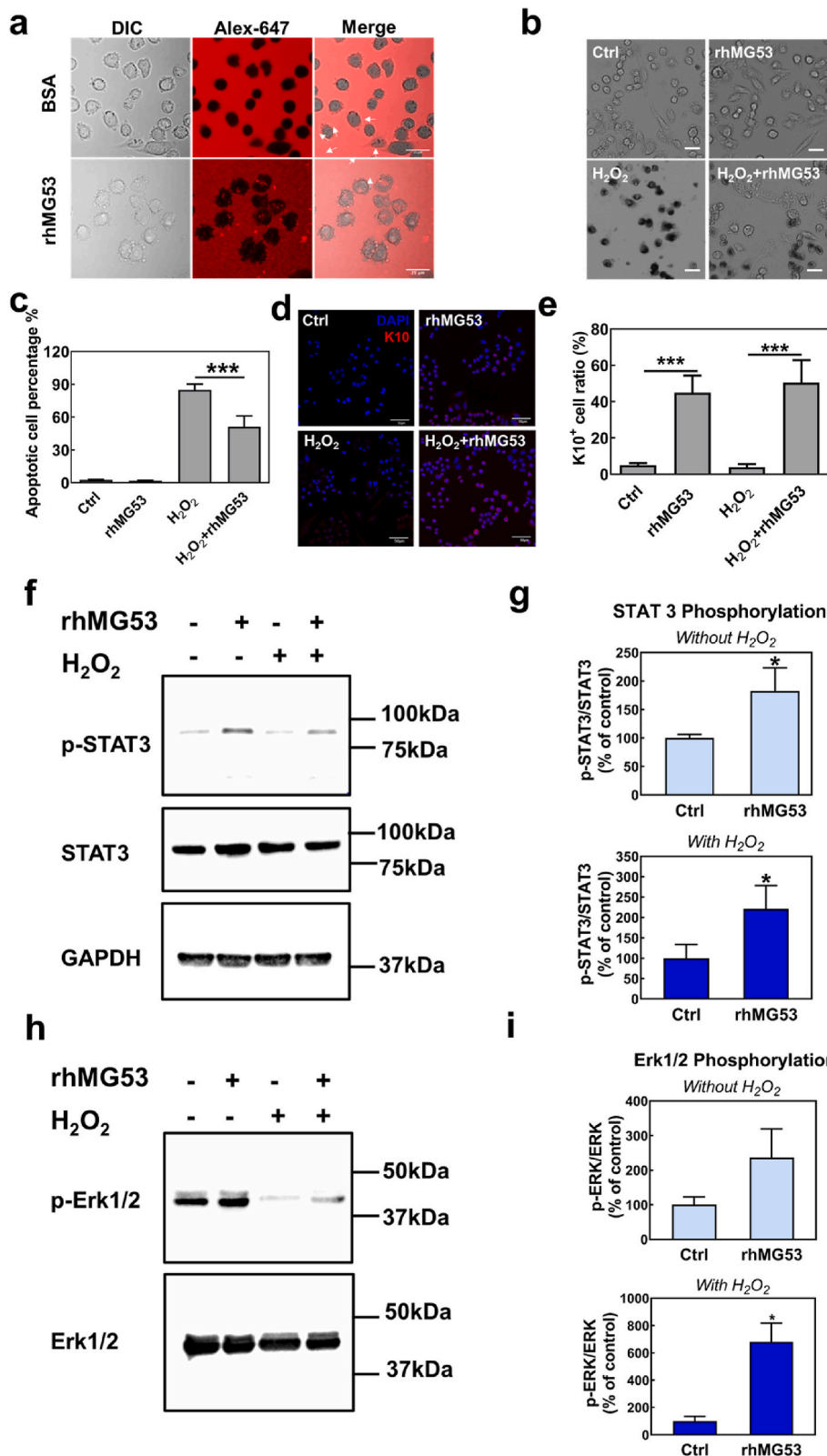


**Fig. 3.** Uptake of rhMG53 by HFSCs and it decreased apoptosis of HFSC and increased HFSCs differentiation into keratinocytes under oxidative stress. **a.** rhMG53 uptake by HFSCs. HFSCs were treated with Alex647-labeled rhMG53 (red) or Alex647 labeled BSA (control). Confocal images were taken from 60 min treated cells. Arrows indicate rhMG53 uptake in the cells. **b, c.** TUNEL staining showed rhMG53 suppressed HFSCs apoptosis under H<sub>2</sub>O<sub>2</sub> (n  $\geq$  6, \*\*\*p < 0.001). **d, e.** HFSCs differentiation into keratinocytes and quantification of K10<sup>+</sup> cells. Scale bar = 50  $\mu\text{m}$  (n = 5, \*\*\*p < 0.001). **f, g.** Western blotting of p-STAT3, STAT3 and GAPDH expression and derived from HFSCs. HFSCs were treated with serum-free medium (control), H<sub>2</sub>O<sub>2</sub>, rhMG53, and rhMG53 with H<sub>2</sub>O<sub>2</sub> (n = 4). **h, i.** Western blotting of p-Erk1/2 and Erk1/2 expressed from HFSCs (n = 4, \*p < 0.05).

enter into HFSCs. After incubating HFSCs with rhMG53 (Alex647 labeled) for only ~10 min, the protein began to aggregate on the cell membrane (Fig. 3a). Following 60 min of incubation, rhMG53 was found to be inside the cells (Fig. 3a). In contrast, control protein BSA was not taken up by the cells.

We determined the effect of rhMG53 on HFSC apoptosis in the presence of H<sub>2</sub>O<sub>2</sub>. As shown in Fig. 3b and c, HFSCs experienced massive cell death under H<sub>2</sub>O<sub>2</sub>. The treatment with rhMG53 significantly reduced cell apoptosis from 84.8% to 51.2% (p < 0.001).

Previous studies showed that the HFSCs are the major reservoir of adult stem cells [18], which play a crucial role in wound healing [21].

We next investigated how rhMG53 affected the differentiation of HFSCs under H<sub>2</sub>O<sub>2</sub> condition. The cells were cultured in the growth medium supplemented with 500 μM H<sub>2</sub>O<sub>2</sub>. After 24 h of culture, the HFSCs in the group without rhMG53 did not express K10, a maker for keratinocytes [55]. Addition of rhMG53 significantly promoted the differentiation (Fig. 3d and e). We also found that rhMG53 was able to induce differentiation of HFSCs into keratinocytes under basal condition without H<sub>2</sub>O<sub>2</sub> treatment. Moreover, rhMG53 treatment could promote HFSC differentiation under H<sub>2</sub>O<sub>2</sub> condition. These findings indicated that rhMG53 can enter into cells and promote HFSCs survival and differentiation under oxidative stress.

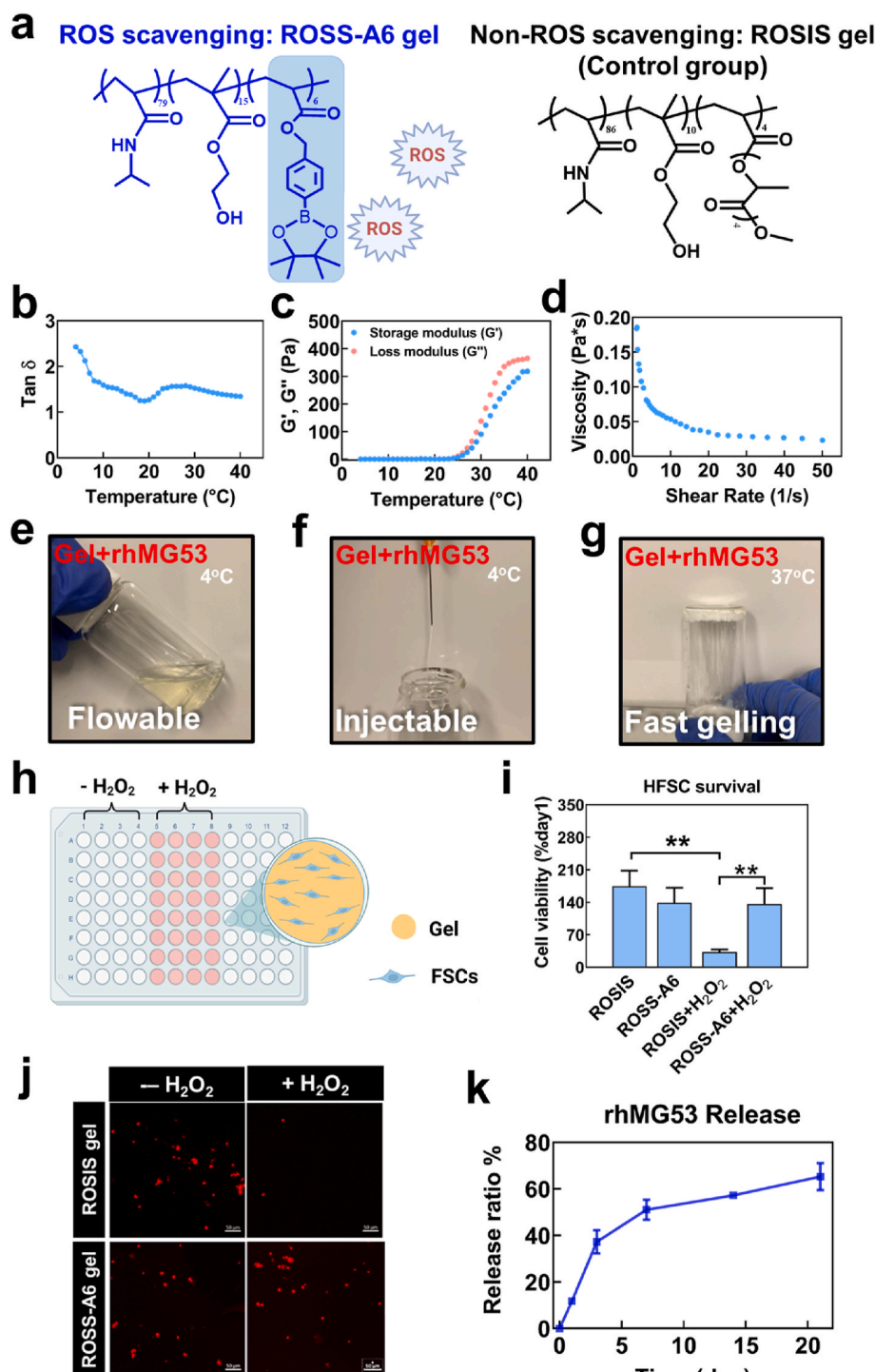


**Fig. 4.** ROS scavenging gel (ROSS-A6) promoted HFSCs survival under oxidative stress. **a.** Structure of poly (NIPAAm<sub>79</sub>-co-HEMA<sub>15</sub>-co-AHPPE<sub>6</sub>) (ROSS-A6 gel) and poly (NIPAAm-co-HEMA-co-APLA) (ROSSIS gel, control gel). **b.**  $\tan \delta$  of the hydrogel solution from 4 °C to 40 °C tested by HR-20 Rheometer. **c.** The storage modulus (G') and the loss modulus (G'') of the hydrogel solution from 4 °C to 40 °C. **d.** Viscosity of the hydrogel tested at 4 °C with shear rate ramping from 1 to 50 s<sup>-1</sup>. **e, f, g.** Encapsulation of MG53 in ROSS-A6 gel. The mixture solution was flowable (**e**) and injectable (**f**) at 4 °C, and it can quickly form solid gel at 37 °C (**g**). **h.** Schematic illustration of a 2D cell culture model with MG53/Gel/HFSCs with and without H<sub>2</sub>O<sub>2</sub>. **i.** HFSCs survival on gel at different time points examined by MTT assay. **j.** Live cell images illustrated that ROS responsive ROSS-A6 gel enhanced HFSCs survival rate under oxidative stress compared with non-ROS responsive ROSIS gel (\*p < 0.05). HFSCs were pre-labeled with live cell tracker CMDil (red) and imaged by confocal microscopy with Z-stack mode at day 5. Scale bar = 50 μm. **k.** *In vitro* release kinetics of MG53 in ROSS-A6 gel for 21 days (n = 6).



### 3.4. rhMG53 suppresses H<sub>2</sub>O<sub>2</sub>-induced HFSCs apoptosis via STAT3 and MAPK/Erk1/2 signaling

STAT3 signaling was reported to play a critical role in the survival of epidermal cells [56]. To investigate whether rhMG53-enhanced HFSCs survival under oxidative stress was associated with STAT3 signaling, Western blot was performed for HFSCs with or without being treated by rhMG53 in the presence of H<sub>2</sub>O<sub>2</sub> (Fig. 3f). The phosphorylation of STAT3 was significantly upregulated after treatment with rhMG53 (Fig. 3g).

Erk1/2 is one of the main cascades in mitogen-activated protein kinases (MAPK) signaling pathway linked to the survival of skin cells such as keratinocytes, and dermal fibroblasts [57]. We studied the effect of rhMG53 on the phosphorylation of Erk1/2 (p-Erk1/2) when HFSCs were cultured under oxidative stress. H<sub>2</sub>O<sub>2</sub> significantly reduced the p-Erk1/2 expression ( $p < 0.05$ , Fig. 3h and i), which explained the higher apoptosis rate of HFSCs under oxidative stress. In contrast, rhMG53 treatment significantly enhanced the expression of p-Erk1/2 under H<sub>2</sub>O<sub>2</sub> condition. These results demonstrated that rhMG53 activated both STAT3 and Erk1/2 signaling, leading to increased cell survival under oxidative stress.

### 3.5. ROS-scavenging hydrogel is capable of gradually releasing rhMG53, and enhancing HFSCs survival under oxidative stress

To take advantage of the functions of rhMG53 for enhanced hair follicle development and wound closure, we developed an rhMG53 delivery system based on an injectable, fast gelling, and ROS-scavenging hydrogel ROSS-A6 gel. The hydrogel was synthesized from NIPAAm, HEMA, and AHPPE (Fig. 4a). The NIPAAm and HEMA components were used to provide thermo-sensitivity and increase hydrogel hydrophilicity, respectively. AHPPE was used to scavenge upregulated ROS in the diabetic wounds. Upon oxidization of 4-(hydroxymethyl)-phenylboronic acid pinacol ester in the AHPPE component by ROS, the component becomes acrylic acid component and releases soluble boronic acid. We have demonstrated in the previous study that AHPPE-containing polymers were able to effectively scavenge superoxide, hydroxyl radical, and H<sub>2</sub>O<sub>2</sub> [38].

The hydrogel solution had a sol-gel transition temperature of 19 °C based on the relationship of loss factor  $\tan\delta$  and temperature (Fig. 4b). The hydrogel experienced a steep increase of both storage modulus ( $G'$ ) and loss modulus ( $G''$ ) starting from 25 °C, and reached 279.7 Pa and 354.9 Pa at 37 °C, respectively (Fig. 4c). The hydrogel exhibited shear-thinning behavior. The viscosity of the hydrogel solution decreased when the shear rate was increased (Fig. 4d).

The mixture of rhMG53 and ROSS-A6 gel solution was flowable at 4 °C (Fig. 4e). It can be readily injected through a 27G needle typically used for tissue injection (Fig. 4f). At 37 °C, the mixture solidified within 6 s to form a soft hydrogel (Fig. 4g). The fast gelation property is advantageous for wound healing application, as the delivered mixture can quickly solidify, allowing for efficient retainment of rhMG53 protein in the wound site.

We first studied whether ROSS-A6 gel can promote HFSCs survival under oxidative stress by scavenging ROS. HFSCs were cultured on the surface of the hydrogel in the presence or absence of H<sub>2</sub>O<sub>2</sub> (Fig. 4h). ROS-insensitive hydrogel (ROSIS gel) was synthesized and used as a control (Fig. 4a). After 5 days of culture without H<sub>2</sub>O<sub>2</sub>, HFSCs exhibited similar viability in both ROSS-A6 gel and ROSIS gel. Addition of H<sub>2</sub>O<sub>2</sub> during the culture led to 67.1% cell death in the ROSIS gel group, whereas the HFSC survival was significantly enhanced in the ROSS-A6 gel group (Fig. 4i and j). These results demonstrated that the ROSS-A6 gel was able to protect HFSCs from cell death under oxidative stress. Other synthetic hydrogels have been engineered to regulate chronic wound healing by lowering ROS level [58–60]. However, these studies did not show that the hydrogels can promote survival of stem cells in the skin. Use of ROS-scavenging hydrogel to develop rhMG53 delivery system is advantageous as both rhMG53 and ROSS-gel can improve

HFSC survival. In addition, even after rhMG53 is completely released, the remaining hydrogel can continue to improve HFSC survival by scavenging ROS in the wounds.

To quantify the sustained release capability of rhMG53 encapsulated in the ROSS-A6 gel, the mixture was incubated in 37 °C DPBS for 21 days. As shown in Fig. 4k, sustained release of rhMG53 was observed in the 21-day period. After 21 days, 65.3% of the initial amount was released. The release was relatively faster in the first 3 days, followed by a slower and relatively linear release from day 7 to day 21. The sustained rhMG53 release from ROSS-A6 likely reflects the hydrogen bonding between the rhMG53 and the hydrogel, which protected the protein from quick release. It is expected that rhMG53 will be able to continuously release from the hydrogel after 21 days until all of the protein is released. After applying into diabetic wounds, the release rate will be higher than *in vitro* since the ROS-responsive 4-(hydroxymethyl)-phenylboronic acid pinacol ester will allow the hydrogel to degrade faster in the ROS-rich wounds.

### 3.6. Sustained release of rhMG53 accelerates wound closure and hair follicle development in diabetic wounds

Diabetic wounds have a slow healing rate. We used *db/db* mice and *db/+* mice to show the impaired diabetic wound healing (Fig. 5a). We found that the wound size in *db/db* mice without treatment remained 54.5% after 12 days. In contrast, the *db/+* mice without treatment showed a much faster healing rate with complete wound closure at day 12 (Fig. 5b and c). Repetitive administration of rhMG53 through saline to the diabetic wounds for 3 consecutive days significantly enhanced wound closure, where the wound size was decreased to 31.4% at day 12.

As MG53 has a short half-life *in vivo* [33], we reasoned that sustained release of rhMG53 from hydrogel would accelerate wound closure. In addition, ROSS-A6 may scavenge ROS in the wounds, which can further improve diabetic wound closure. We thus investigated the effect of the rhMG53 delivery system on wound healing in the *db/db* mice (Fig. 6a). The wounds treated with ROSS-A6 gel only was used as control. As expected, the *db/db* mice that treated with ROSS-A6 gel alone demonstrated a substantially faster healing rate with an average wound size of 41.7% on day 12, compared to the no treatment group that left with an average wound size of 54.5% at the same time point (Fig. 6b and c). Notably, the *db/db* mice that received a single dose of rhMG53 delivery system (rhMG53/ROSS-A6 group) healed significantly faster than those treated with ROSS-A6 gel alone (Fig. 6c,  $p < 0.001$  on day 12), and than those had 3 doses of rhMG53/saline (Fig. 5c,  $p < 0.001$  on day 12). These results are consistent with *in vitro* studies where rhMG53 promoted survival and differentiation of HFSCs (Fig. 3b, c, d, and e). When observed at day 22, the wounds in both ROSS-A6 and rhMG53/ROSS-A6 groups were completely closed.

Epidermis thickness changes at different stage of wound healing [61]. We assessed thickness of the epidermis in the closed region of wounds at days 8 and 22, respectively. The two time points represent the middle and end stages of wound healing. At day 8, the epidermis thickness in the rhMG53/ROSS-A6 and ROSS-A6 groups was significantly greater than that in the No-treatment group. The highest thickness was found for the rhMG53/ROSS-A6 group. These results demonstrated that the released rhMG53 and ROS-sensitive hydrogel accelerated the re-epithelialization (Fig. 6d and e). At day 22 when the wounds were completely closed, the epidermis thickness in the rhMG53/ROSS-A6 and ROSS-A6 groups was significantly reduced compared to that at day 8. This thickness in the rhMG53/ROSS-A6 group ( $65.7 \pm 10.8 \mu\text{m}$ ) was closer to the thickness of unwounded skin of *db/db* mice [38].

Notably, the enhanced wound closure by rhMG53 delivery system did not lead to fibrosis as the collagen deposition was significantly lower in the rhMG53/ROSS-A6 group at day 22 (Fig. 6f). The rhMG53 delivery system also significantly promoted hair follicle development. At days 8 and 22, the rhMG53/ROSS-A6 group exhibited the highest density of

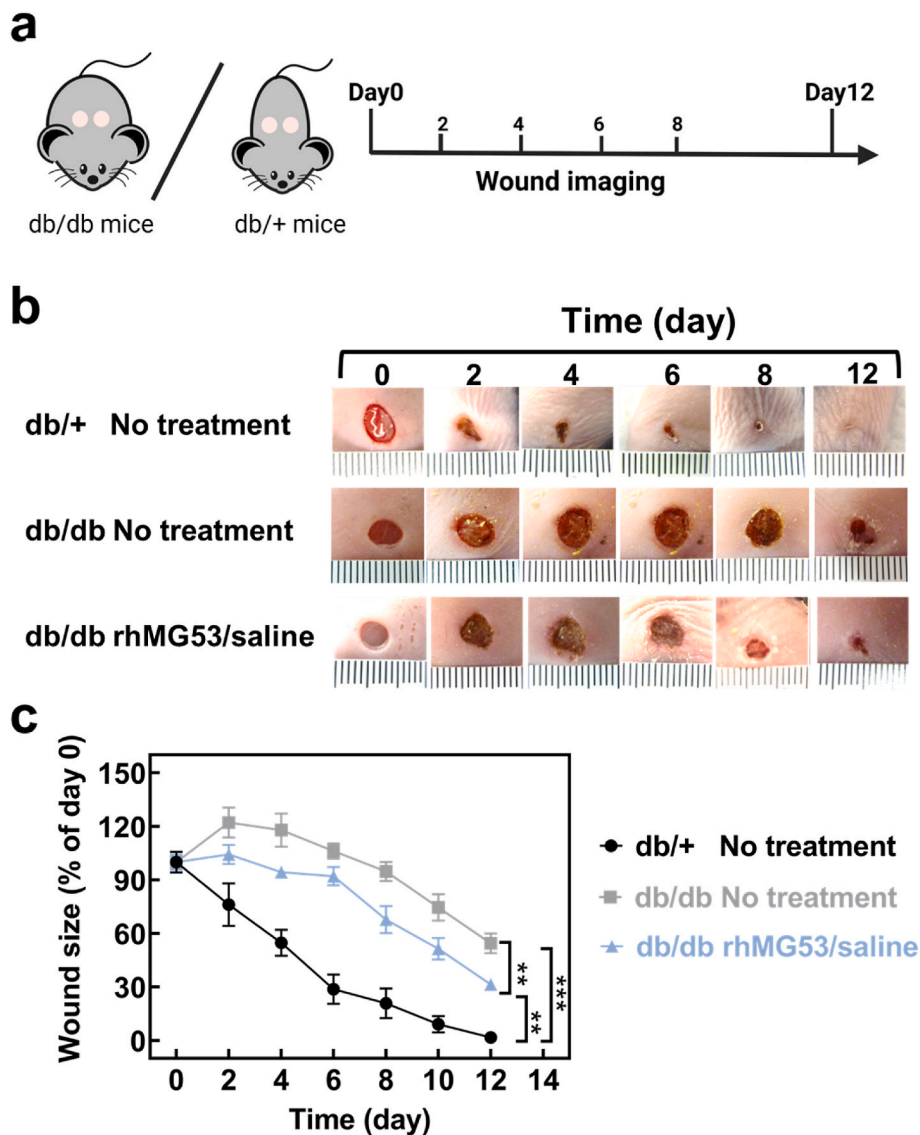


**Fig. 5. Delayed chronic wound healing in diabetic (*db/db*) mice and limited efficacy with the injection of rhMG53/saline. a.** Schematic illustration of the design of animal experiments to test the delayed wound healing of *db/db* mice and therapeutic effect of MG53. **b.** Representative images of wounds taken at different time points. Wounds were created using 5 mm Biopsy punches on the back of *db/+* mice and *db/db* mice. MG53/saline was injected subcutaneously on the back. Wound healing on *db/db* mice showed a significant delay compared to *db/+* mice 12 days after wounding. The injection of MG53 showed limited efficacy in wound healing. **c.** Wound closure rate for 12 days for each treatment category. Wound size ratios were normalized to day 0, data were expressed as means  $\pm$  standard error ( $n = 8$  for days 0–4, and  $n = 6$  for days 6–12,  $**p < 0.01$ ,  $***p < 0.001$ ).

$K14^+$  hair follicles compared to the ROSS-A6 and No-treatment groups (Fig. 6g and h). In addition, the ROSS-A6 alone also promoted hair follicle development. Hair follicle is a major skin appendage associated with epidermal homeostasis and wound repair. It displays a dynamic, life-long cycling process (hair generation) including anagen (rapid growth), catagen (apoptosis driven regression) and telogen (relative resting) [1]. Hair follicle loss is often accompanied by the termination of hair cycling and comprised wound healing [62]. Our results demonstrate that rhMG53 enhances hair follicle development and hair regeneration, and thus contributes to accelerated wound healing.

Collectively, this work demonstrates that MG53 plays an important role in the healing of diabetic wounds including wound closure and hair follicle development (Fig. 7). Sustained delivery of rhMG53 by controlled release significantly promoted diabetic wound healing in *db/db* mice (Fig. 7), by enhancing hair follicle stem cell survival and proliferation under oxidative stress, and scavenging ROS in the wounds. Future work will test efficacy of the developed rhMG53 delivery system in large animal models such as diabetic porcine model.

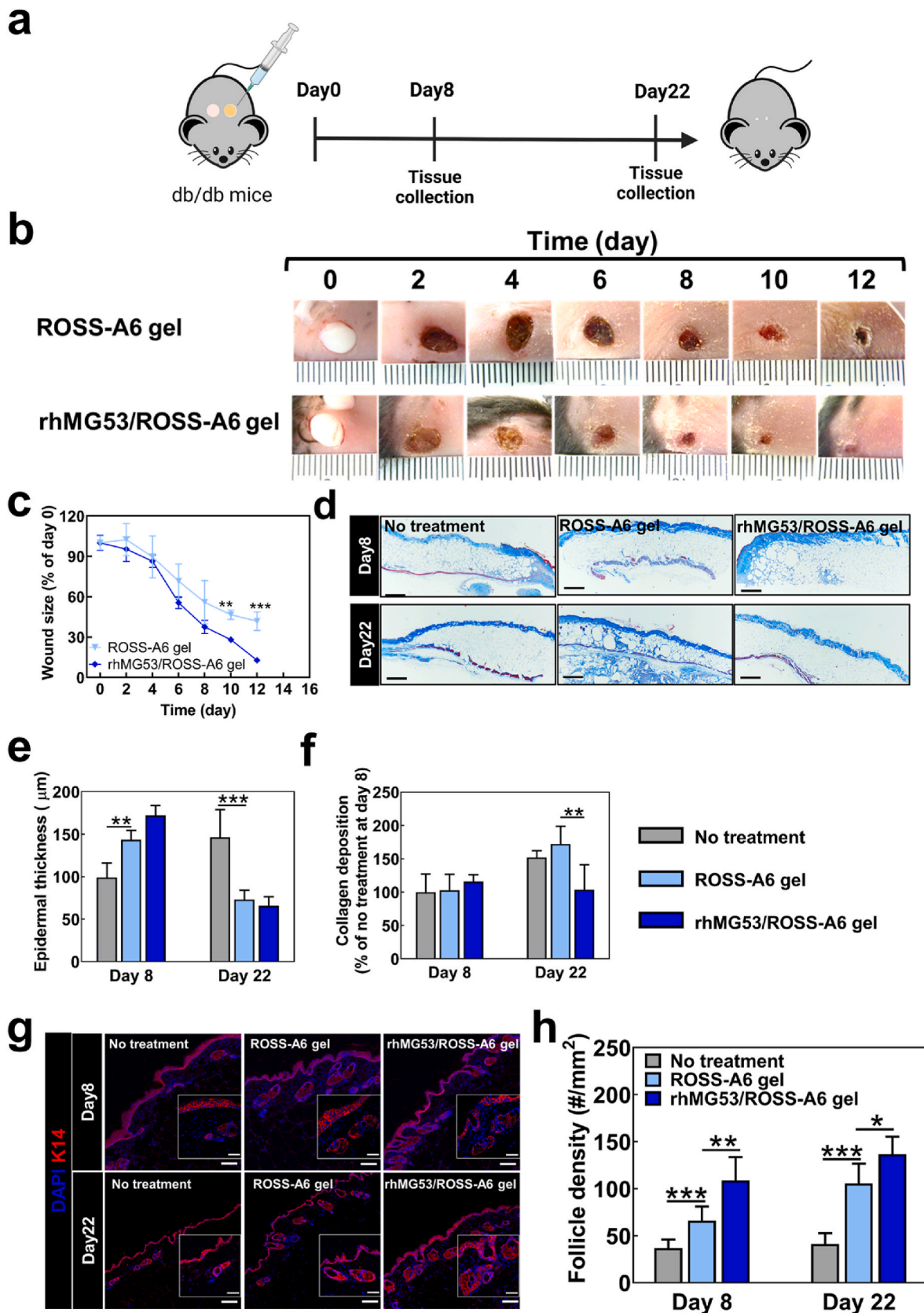
#### 4. Conclusion

In this work, we showed that MG53 contributes to hair follicle development. Genetic ablation of MG53 led to abnormal hair follicle

structure. *In vitro* studies revealed that MG53 is capable of enhancing hair follicle stem cell survival and differentiation under oxidative stress condition existing in the diabetic wounds. Delivery of rhMG53 using an injectable, thermosensitive and ROS-scavenging hydrogel accelerated wound healing and hair follicle development in *db/db* mice.

#### Author contributions

Hong Niu, Conducted most experiments constituting the manuscript, Prepared and wrote the manuscript, Haichang Li, Developed the concept for the studies, Conducted most experiments constituting the manuscript, Prepared and wrote the manuscript, Ya Guan, Conducted most experiments constituting the manuscript, Prepared and wrote the manuscript, Zhongguang Li, Contributed their expertise in immunofluorescent staining, living-cell imaging and cell lineage tracking study, Serana Li Zhao, Contributed their expertise in immunofluorescent staining, living-cell imaging and cell lineage tracking study, Peng Chen, Contributed their expertise in immunofluorescent staining, living-cell imaging and cell lineage tracking study, Tao Tan, Performed toxicological studies of rhMG53, Hua Zhu, Contributed their expertise in immunofluorescent staining, living-cell imaging and cell lineage tracking study, Jianjie Ma, Developed the concept for the studies, Prepared and wrote the manuscript, Jianjun Guan, Developed the concept



(caption on next page)



**Fig. 6.** rhMG53/ROSS-A6 gel accelerated *db/db* wound healing with enhanced epidermal thickness and improved formation of hair follicle *in vivo*. **a.** Schematic illustration of the design of animal experiments to test the therapeutic effect of MG53/ROSS-A6 gel in a *db/db* mouse model. **b.** Representative images of wounds taken at different time points. The wounds were treated with ROSS-A6 gel, and MG53/ROSS-A6 gel via subcutaneous injection. rhMG53/ROSS-A6 gel significantly accelerated wound healing compared with the gel group lacking MG53. **c.** Wound closure for 12 days for each treatment category. Wound size ratios were normalized to day 0. Data were expressed as means  $\pm$  standard error ( $n \geq 6$ ,  $**p < 0.01$ ,  $***p < 0.001$ ). **d.** Representative images of Masson trichrome staining (MTS) at day 8 and day 22. Scale bar = 500  $\mu\text{m}$ . **e.** Quantification of epidermal thickness from MTS images at day 8 and day 22. **f.** Quantification of collagen deposition at two time points. **g.** Cytokeratin 14 (K14) staining (10X and 40X) illustrated significantly promoted HFSCs density at both day 8 and day 22 in gel group compared with no treatment group. MG53/ROSS-A6 gel group showed an additional increase of HFSCs density at day 8. Scale bar = 100  $\mu\text{m}$  in lower magnification images. Scale bar = 40  $\mu\text{m}$  in higher magnification inserts. **h.** Quantification of hair follicle density *in vivo* based on the images. ( $n = 8$ ,  $*p < 0.05$ ,  $**p < 0.01$ ,  $***p < 0.001$ ).

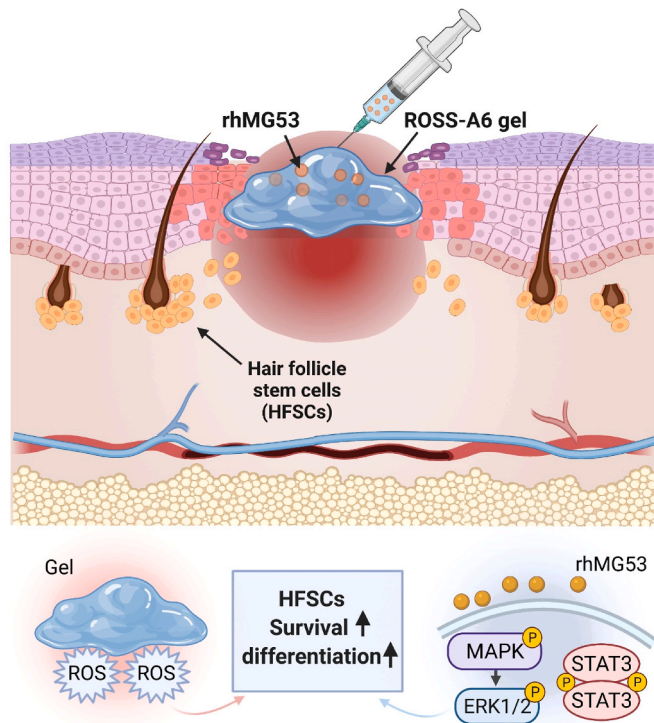


**Fig. 7.** Schematic illustration of accelerated wound healing by the delivery system of rhMG53/ROSS-A6 gel.

for the studies, Prepared and wrote the manuscript.

### Declaration of competing interest

J. M. and T. T. are co-founders of TRIM-edicine, which develops rhMG53 for treatment of human disease. Patents on the use of rhMG53 are held by Rutgers University and Ohio State University.

### Acknowledgments

This work was supported by National Institutes of Health (R01AG056919). It was also supported by the OSU Lockwood Early Career Development Award to H.L.

### References

- [1] C.K. Sen, Wound healing essentials: let there be oxygen, *Wound Repair Regen.* 17 (1) (2009) 1–18.
- [2] M.K. Henzel, K.M. Bogie, M. Guihan, C.H. Ho, Pressure ulcer management and research priorities for patients with spinal cord injury: consensus opinion from SCI QUERI Expert Panel on Pressure Ulcer Research Implementation, *J. Rehabil. Res. Dev.* 48 (3) (2011) xi–xxxii.
- [3] S. Tojkander, G. Gateva, P. Lappalainen, Actin stress fibers—assembly, dynamics and biological roles, *J. Cell Sci.* 125 (Pt 8) (2012) 1855–1864.
- [4] P. Martin, Wound healing—aiming for perfect skin regeneration, *Science* 276 (5309) (1997) 75–81.
- [5] G. Gabbiani, The myofibroblast in wound healing and fibrocontractive diseases, *J. Pathol.* 200 (4) (2003) 500–503.
- [6] B. Hinz, Formation and function of the myofibroblast during tissue repair, *J. Invest. Dermatol.* 127 (3) (2007) 526–537.
- [7] G.C. Gurtner, S. Werner, Y. Barrandon, M.T. Longaker, Wound repair and regeneration, *Nature* 453 (7193) (2008) 314–321.
- [8] N.S. Greaves, K.J. Ashcroft, M. Baguneid, A. Bayat, Current understanding of molecular and cellular mechanisms in fibroplasia and angiogenesis during acute wound healing, *J. Dermatol. Sci.* 72 (3) (2013) 206–217.
- [9] M. Schäfer, S. Werner, Transcriptional control of wound repair, *Annu. Rev. Cell Dev. Biol.* 23 (2007) 69–92.
- [10] L.M. Sun, Y.J. Huang, Z.H. Bian, J. Petrosino, Z. Fan, Y.Z. Wang, K.H. Park, T. Yue, M. Schmidt, S. Galster, J.J. Ma, H. Zhu, M.J. Zhang, Sundew-inspired adhesive hydrogels combined with adipose-derived stem cells for wound healing, *ACS Appl. Mater. Inter.* 8 (3) (2016) 2423–2434.
- [11] M.I. Morasso, M. Tomic-Canic, Epidermal stem cells: the cradle of epidermal determination, differentiation and wound healing, *Biol. Cell.* 97 (3) (2005) 173–183.
- [12] R. Yang, F. Liu, J. Wang, X. Chen, J. Xie, K. Xiong, Epidermal stem cells in wound healing and their clinical applications, *Stem Cell Res. Ther.* 10 (1) (2019) 1–14.
- [13] S. Dekoninck, C. Blanpain, Stem cell dynamics, migration and plasticity during wound healing, *Nat. Cell Biol.* 21 (1) (2019) 18–24.
- [14] Y. Shen, L. Dai, X. Li, R. Liang, G. Guan, Z. Zhang, W. Cao, Z. Liu, S. Mei, W. Liang, Epidermal stem cells cultured on collagen-modified chitin membrane induce in situ tissue regeneration of full-thickness skin defects in mice, *PLoS One* 9 (2) (2014), e87557.
- [15] T. Tumber, G. Guasch, V. Greco, C. Blanpain, W.E. Lowry, M. Rendl, E. Fuchs, Defining the epithelial stem cell niche in skin, *Science* 303 (5656) (2004) 359–363.
- [16] G. Taylor, M.S. Lehrer, P.J. Jensen, T.T. Sun, R.M. Lavker, Involvement of follicular stem cells in forming not only the follicle but also the epidermis, *Cell* 102 (4) (2000) 451–461.
- [17] F. Heidari, A. Yari, H. Rasoolijazi, M. Soleimani, A. Dehpoor, N. Sajedi, S.V. Joulai, M. Nobakht, Bulge hair follicle stem cells accelerate cutaneous wound healing in rats, *Wounds: Compendium. Clin. Res. Prac.* 28 (4) (2016) 132–141.
- [18] W.M. Woo, A.E. Oro, Snapshot: hair follicle stem cells, *Cell* 146 (2) (2011) 334–334 e2.
- [19] C.C. Yang, G. Cotsarelis, Review of hair follicle dermal cells, *J. Dermatol. Sci.* 57 (1) (2010) 2–11.
- [20] F. Jimenez, C. Garde, E. Poblet, B. Jimeno, J. Ortiz, M.L. Martinez, A. Gutierrez-Rivera, V. Perez-Lopez, U. Etxaniz, C. Naveda, J.L. Higuera, N. Egues, E. Escario, A. Izeta, A pilot clinical study of hair grafting in chronic leg ulcers, *Wound Repair Regen. : official publication of the Wound Healing Society [and] the European Tissue Repair Society* 20 (6) (2012) 806–814.
- [21] M. Ito, Y. Liu, Z. Yang, J. Nguyen, F. Liang, R.J. Morris, G. Cotsarelis, Stem cells in the hair follicle bulge contribute to wound repair but not to homeostasis of the epidermis, *Nat. Med.* 11 (12) (2005) 1351–1354.
- [22] C.K. Sen, S. Roy, Redox signals in wound healing, *Biochim. Biophys. Acta Gen. Subj.* 1780 (11) (2008) 1348–1361.
- [23] G. Buonocore, S. Perrone, M.L. Tataranno, Oxygen Toxicity: Chemistry and Biology of Reactive Oxygen Species, *Seminars in Fetal and Neonatal Medicine*, Elsevier, 2010, pp. 186–190.
- [24] M. Lotfy, J. Adegate, H. Kalasz, J. Singh, E. Adegate, Chronic complications of diabetes mellitus: a mini review, *Curr. Diabetes Rev.* 13 (1) (2017) 3–10.
- [25] C. Cai, H. Masumiya, N. Weisleder, N. Matsuda, M. Nishi, M. Hwang, J.-K. Ko, P. Lin, A. Thornton, X. Zhao, MG53 nucleates assembly of cell membrane repair machinery, *Nat. Cell Biol.* 11 (1) (2009) 56–64.
- [26] Y. Jia, K. Chen, P. Lin, G. Lieber, M. Nishi, R. Yan, Z. Wang, Y. Yao, Y. Li, B. A. Whitson, P. Duann, H. Li, X. Zhou, H. Zhu, H. Takeshima, J.C. Hunter, R. L. McLeod, N. Weisleder, C. Zeng, J. Ma, Treatment of acute lung injury by targeting MG53-mediated cell membrane repair, *Nat. Commun.* 5 (2014) 4387.
- [27] P. Duann, H. Li, P. Lin, T. Tan, Z. Wang, K. Chen, X. Zhou, K. Gumpfer, H. Zhu, T. Ludwig, MG53-mediated cell membrane repair protects against acute kidney injury, *Sci. Transl. Med.* 7 (279) (2015), 279ra36–279ra36.
- [28] C. Cai, H. Masumiya, N. Weisleder, N. Matsuda, M. Nishi, M. Hwang, J.K. Ko, P. Lin, A. Thornton, X. Zhao, Z. Pan, S. Komazaki, M. Brotto, H. Takeshima, J. Ma, MG53 nucleates assembly of cell membrane repair machinery, *Nat. Cell Biol.* 11 (1) (2009) 56–64.
- [29] C. Cai, H. Masumiya, N. Weisleder, Z. Pan, M. Nishi, S. Komazaki, H. Takeshima, J. Ma, MG53 regulates membrane budding and exocytosis in muscle cells, *J. Biol. Chem.* 284 (5) (2009) 3314–3322.
- [30] C. Cai, N. Weisleder, J.K. Ko, S. Komazaki, Y. Sunada, M. Nishi, H. Takeshima, J. Ma, Membrane repair defects in muscular dystrophy are linked to altered

- interaction between MG53, caveolin-3, and dysferlin, *J. Biol. Chem.* 284 (23) (2009) 15894–15902.
- [31] Q. Wang, Z. Bian, Q. Jiang, X. Wang, X. Zhou, K.H. Park, W. Hsueh, B.A. Whitson, E. Haggard, H. Li, K. Chen, C. Cai, T. Tan, H. Zhu, J. Ma, MG53 does not manifest the development of diabetes in db/db mice, *Diabetes* 69 (5) (2020) 1052–1064.
- [32] M. Sermersheim, A.D. Kenney, P.H. Lin, T.M. McMichael, C. Cai, K. Gumpfer, T.M. A. Adesanya, H. Li, X. Zhou, K.H. Park, J.S. Yount, J. Ma, MG53 suppresses interferon-beta and inflammation via regulation of ryanodine receptor-mediated intracellular calcium signaling, *Nat. Commun.* 11 (1) (2020) 3624.
- [33] N. Weisleder, N. Takizawa, P. Lin, X. Wang, C. Cao, Y. Zhang, T. Tan, C. Ferrante, H. Zhu, P.J. Chen, R. Yan, M. Sterling, X. Zhao, M. Hwang, M. Takeshima, C. Cai, H. Cheng, H. Takeshima, R.P. Xiao, J. Ma, Recombinant MG53 protein modulates therapeutic cell membrane repair in treatment of muscular dystrophy, *Sci. Transl. Med.* 4 (139) (2012), 139ra85.
- [34] P. Duann, H. Li, P. Lin, T. Tan, Z. Wang, K. Chen, X. Zhou, K. Gumpfer, H. Zhu, T. Ludwig, P.J. Mohler, B. Rovin, W.T. Abraham, C. Zeng, J. Ma, MG53-mediated cell membrane repair protects against acute kidney injury, *Sci. Transl. Med.* 7 (279) (2015), 279ra36.
- [35] Y. Gao, Z. Li, J. Huang, M. Zhao, J. Wu, In situ formation of injectable hydrogels for chronic wound healing, *J. Math. Chem.* B 8 (38) (2020) 8768–8780.
- [36] N. Asadi, H. Pazoki-Toroudi, A.R. Del Bakhshayesh, A. Akbarzadeh, S. Davaran, N. Annabi, Multifunctional hydrogels for wound healing: special focus on biomacromolecular based hydrogels, *Int. J. Biol. Macromol.* 170 (2021) 728–750.
- [37] H. Li, P. Duann, P.H. Lin, L. Zhao, Z. Fan, T. Tan, X. Zhou, M. Sun, M. Fu, M. Orange, M. Sermersheim, H. Ma, D. He, S.M. Steinberg, R. Higgins, H. Zhu, E. John, C. Zeng, J. Guan, J. Ma, Modulation of wound healing and scar formation by MG53 protein-mediated cell membrane repair, *J. Biol. Chem.* 290 (40) (2015) 24592–24603.
- [38] Y. Guan, H. Niu, Z. Liu, Y. Dang, J. Shen, M. Zayed, L. Ma, J. Guan, Sustained oxygenation accelerates diabetic wound healing by promoting epithelialization and angiogenesis and decreasing inflammation, *Sci. Adv.* 7 (35) (2021), eabj0153.
- [39] A. Amitai-Lange, A. Altshuler, J. Bublely, N. Dbayat, B. Tiosano, R. Shalom-Feuerstein, Lineage tracing of stem and progenitor cells of the murine corneal epithelium, *Stem Cell.* 33 (1) (2015) 230–239.
- [40] E. Roy, Z. Neufeld, L. Ceron, H.Y. Wong, S. Hodgson, J. Livet, K. Khosrotehrani, Bimodal behaviour of interfollicular epidermal progenitors regulated by hair follicle position and cycling, *EMBO J.* 35 (24) (2016) 2658–2670.
- [41] Z.H. Bian, Q. Wang, X.Y. Zhou, T. Tan, K.H. Park, H.F. Kramer, A. McDougal, N. J. Laping, S. Kumar, T.M.A. Adesanya, M. Sermersheim, R. Yi, X.X. Wang, J.W. Wu, K. Gumpfer, Q.W. Jiang, D.F. He, P.H. Lin, H.C. Li, F.X. Guan, J.S. Zhou, M.J. Kohr, C.Y. Zeng, H. Zhu, J.J. Ma, Sustained elevation of MG53 in the bloodstream increases tissue regenerative capacity without compromising metabolic function, *Nat. Commun.* 10 (2019).
- [42] Z. Fan, Z. Xu, H. Niu, N. Gao, Y. Guan, C. Li, Y. Dang, X. Cui, X.L. Liu, Y. Duan, An injectable oxygen release system to augment cell survival and promote cardiac repair following myocardial infarction, *Sci. Rep.* 8 (1) (2018) 1371.
- [43] H. Niu, X. Li, H. Li, Z. Fan, J. Ma, J. Guan, Thermosensitive, fast gelling, photoluminescent, highly flexible, and degradable hydrogels for stem cell delivery, *Acta Biomater.* 83 (2019) 96–108.
- [44] H. Niu, C. Li, Y. Guan, Y. Dang, X. Li, Z. Fan, J. Shen, L. Ma, J. Guan, High oxygen preservation hydrogels to augment cell survival under hypoxic condition, *Acta Biomater.* 105 (2020) 56–67.
- [45] J. Van Meerloo, G.J. Kaspers, J. Cloos, *Cell Sensitivity Assays: the MTT Assay*, Cancer cell culture, Springer, 2011, pp. 237–245.
- [46] M. Yanamandala, W. Zhu, D.J. Garry, T.J. Kamp, J.M. Hare, H.W. Jun, Y.S. Yoon, N. Bursac, S.D. Prabhu, G.W. Dorn 2nd, R. Bolli, R.N. Kitsis, J. Zhang, Overcoming the roadblocks to cardiac cell therapy using tissue engineering, *J. Am. Coll. Cardiol.* 70 (6) (2017) 766–775.
- [47] M.V. Plikus, D.L. Gay, E. Treffeisen, A. Wang, R.J. Supapannachart, G. Cotsarelis, Epithelial Stem Cells and Implications for Wound Repair, *Seminars in Cell & Developmental Biology*, Elsevier, 2012, pp. 946–953.
- [48] H. Li, P. Duann, P.-H. Lin, L. Zhao, Z. Fan, T. Tan, X. Zhou, M. Sun, M. Fu, M. Orange, Modulation of wound healing and scar formation by MG53 protein-mediated cell membrane repair, *J. Biol. Chem.* 290 (40) (2015) 24592–24603.
- [49] T.A. Weissman, Y.A. Pan, Brainbow: new resources and emerging biological applications for multicolor genetic labeling and analysis, *Genetics* 199 (2) (2015) 293–306.
- [50] A. Amitai-Lange, A. Altshuler, J. Bublely, N. Dbayat, B. Tiosano, R. Shalom-Feuerstein, Lineage tracing of stem and progenitor cells of the murine corneal epithelium, *Stem Cell.* 33 (1) (2015) 230–239.
- [51] C. Dunnill, T. Patton, J. Brennan, J. Barrett, M. Dryden, J. Cooke, D. Leaper, N. T. Georgopoulos, Reactive oxygen species (ROS) and wound healing: the functional role of ROS and emerging ROS-modulating technologies for augmentation of the healing process, *Int. Wound J.* 14 (1) (2017) 89–96.
- [52] M. Schäfer, S. Werner, Oxidative stress in normal and impaired wound repair, *Pharmacol. Res.* 58 (2) (2008) 165–171.
- [53] C.M. Quinzii, L.C. López, R.W. Gilkerson, B. Dorado, J. Coku, A.B. Naini, C. Lagier-Tourenne, M. Schuelke, L. Salviati, R. Carrozzo, Reactive oxygen species, oxidative stress, and cell death correlate with level of CoQ10 deficiency, *Faseb. J.* 24 (10) (2010) 3733–3743.
- [54] C.L. Bigarella, R. Liang, S. Ghaffari, Stem cells and the impact of ROS signaling, *Development* 141 (22) (2014) 4206–4218.
- [55] I. Goren, Y. Köhler, A. Aglan, J. Pfeilschifter, K.-F. Beck, S. Frank, Increase of cystathionine-γ-lyase (CSE) during late wound repair: hydrogen sulfide triggers cytokeratin 10 expression in keratinocytes, *Nitric Oxide* 87 (2019) 31–42.
- [56] T. Hirano, K. Ishihara, M. Hibi, Roles of STAT3 in mediating the cell growth, differentiation and survival signals relayed through the IL-6 family of cytokine receptors, *Oncogene* 19 (21) (2000) 2548–2556.
- [57] S.-R. Park, J.-W. Kim, H.-S. Jun, J.Y. Roh, H.-Y. Lee, I.-S. Hong, Stem cell secretome and its effect on cellular mechanisms relevant to wound healing, *Mol. Ther.* 26 (2) (2018) 606–617.
- [58] C. Hu, F. Zhang, L. Long, Q. Kong, R. Luo, Y. Wang, Dual-responsive injectable hydrogels encapsulating drug-loaded micelles for on-demand antimicrobial activity and accelerated wound healing, *J. Contr. Release* 324 (2020) 204–217.
- [59] Y. Liang, J. He, B. Guo, Functional hydrogels as wound dressing to enhance wound healing, *ACS Nano* 15 (8) (2021) 12687–12722.
- [60] A. Rasool, S. Ata, A. Islam, Stimuli responsive biopolymer (chitosan) based blend hydrogels for wound healing application, *Carbohydr. Polym.* 203 (2019) 423–429.
- [61] F. Anjum, N.A. Agabalyan, H.D. Sparks, N.L. Rosin, M.S. Kallos, J. Biernaskie, Biocomposite nanofiber matrices to support ECM remodeling by human dermal progenitors and enhanced wound closure, *Sci. Rep.* 7 (1) (2017) 1–17.
- [62] F. Jiménez, C. Garde, E. Poblet, B. Jimeno, J. Ortiz, M.L. Martínez, A. Gutiérrez-Rivera, V. Pérez-López, U. Etxaniz, C. Naveda, A pilot clinical study of hair grafting in chronic leg ulcers, *Wound Repair Regen.* 20 (6) (2012) 806–814.